Crustal differentiation in the early solar system: clues from the unique achondrite Northwest Africa 7325 (NWA 7325)

Jean-Alix J-A Barrat, R. C. Greenwood, A. Verchovsky, Ph Gillet, C Bollinger, Jessica Langlade, Céline C. Liorzou, I.A. Franchi

Crustal differentiation in the early solar system: clues from the unique achondrite Northwest Africa 7325 (NWA 7325).

By

J.A. Barrat[1], R.C. Greenwood[2], A.B. Verchovsky[2], Ph. Gillet[3],

C. Bollinger[4], J.A. Langlade[4], C. Liorzou[1], and I.A. Franchi[2].

1: Université de Bretagne Occidentale, Institut Universitaire Européen de la Mer, CNRS UMR 6538, Place Nicolas Copernic, 29280 Plouzané, France. E-mail: barrat@univ-brest.fr (corresponding author)

2 : Planetary and Space Sciences, Department of Physical Sciences, The Open University, Walton Hall, Milton Keynes, MK7 6AA,United Kingdom.

3 : EPSL, Institute of Condensed Matter Physics, Ecole Polytechnique Fédérale de Lausanne (EPFL), Station 3, CH-1015 Lausanne, Switzerland.

4: CNRS UMS 3113, I.U.E.M., Place Nicolas Copernic, 29280 Plouzané Cedex, France.

Abstract

The unique achondrite NWA 7325 is an unusual olivine gabbro composed chiefly of calcic plagioclase (An_{85-93}), diopsidic pyroxene ($En_{50.1-54.0}$ $Wo_{44.8-49.3}$ $Fs_{0.6-1.3}$), and forsteritic olivine (Fo_{97}). It is Al and Mg-rich and Fe and Na-poor and displays very low concentrations of incompatible trace elements, much below 0.3 x CI abundances for many of them. It is also characterized by huge Eu and Sr anomalies ($Eu/Eu^*=65$, $Sr_n/Ce_n=240$). Although the O isotopic composition of NWA 7325 and some ureilites (those with olivine cores in the range Fo_{75} to Fo_{88}) are similar, a genetic relationship between them is unlikely due to the Fe-poor composition of NWA 7325. It is almost certainly derived from a distinct planetesimal, not previously sampled by other achondrites. The low Na/Al, Ga/Al, Zn/Al ratios as well as the low K, Rb and Cs shown by NWA 7325, suggest a volatile-depleted parent body. This unique gabbro is demonstrably a cumulate, but the composition of its parental melt cannot be precisely assessed. However, the liquid from which NWA 7325 crystallized would have been very poor in incompatible trace elements (Yb in the range of 0.25 to 1.5 x CI abundance) with a very large positive Eu anomaly. Such a melt cannot be the product of the early magmatic activity on a small parent body. Instead, we propose that the parental melt to NWA 7325 formed as a consequence of the total melting of an ancient gabbroic lithology, possibly upon impact, in agreement with the systematics of $^{26}Al-^{26}Mg$. Based on recent dating, the crustal material that was parental to NWA 7325 must have been older than 4562.8 Ma, and formed possibly ≈4566 Ma ago. If this scenario is correct, NWA 7325 provides evidence of one of the earliest crusts on a differentiated body so far studied.

1. Introduction

Achondrites are relatively rare extraterrestrial samples, which comprise only about 4 % of all the recovered meteorites (Meteoritical Bulletin database). Most of them originated from small differentiated bodies, while others were ejected from Mars, or the Moon, and so complement the sampling undertaken during the Apollo and Luna programs. As a result, achondrites have a high scientific value and, therefore, potentially can provide a unique insight into the processes that operated on a variety of differentiated bodies in the early solar system.

The number of parent bodies sampled by achondrites is the subject of ongoing debate. About 95 % of these meteorites originated from only two bodies: 4-Vesta (the howardites, eucrites and diogenites, ca. 1500 meteorites, 75 % of all achondrites) and the now-disrupted ureilite parent body (ca. 400 meteorites, 20 % of all achondrites). Mars, the Moon and a handful of smaller bodies are the sources of the remaining achondrites. Some of them form distinct groups based on their petrographic and isotopic features, such as the aubrites, the angrites or the brachinites (see recent reviews by Keil, 2010, 2012, 2014). Others, as exemplified by Northwest Africa 011 (NWA 011, Yamaguchi et al., 2002), are ungrouped and consequently unique samples of unidentified differentiated bodies. While it is more likely that these unique achondrites originated from one of the many planetesimals that differentiated during the first few million years of solar system history, the possibility that we have in our collections an achondrite from Mercury (e.g., Love and Keil, 1995) cannot be wholly discounted. Such a rock would not only provide essential constraints for models of the differentiation of this planet, but for the chemical structure of the inner solar system too.

The recent discovery of Northwest Africa 7325 (NWA 7325) and its pairing (NWA 8014 and 8486) was stimulating. Thirty seven fragments totaling ca. 600 g, of an unusual achondrite displaying a distinctive green fusion crust (Fig. 1a), were collected near Bir el Abbas, Morocco. Irving et al. (2013) were the first to study this meteorite and to show that it consists of a unique gabbroic lithology. They compared its major element composition to that of Mercury's surface, as determined by the MESSENGER spacecraft (Weider et al., 2012), and suggested that this meteorite could have

76 originated from this planet. Subsequently, this rock has been extensively studied by different teams

77 using a variety of techniques (Irving et al., 2013; Amelin et al., 2013; Bischoff et al., 2013; Sanborn et

78 al., 2013; Dunlap et al., 2014; El Goresy et al., 2014; Goodrich et al., 2014; Jabeen et al., 2014; Kita et

79 al., 2014; Sutton et al., 2014; Weber et al., 2014, 2015; Archer et al., 2015). Although a mercurian

80 origin is not currently favored by most of these studies, this rock remains fascinating and scientifically

81 important by virtue of its distinct petrographic and geochemical features. Here we report new

82 chemical, mineralogical and stable isotope (oxygen, carbon and nitrogen) results that provide

83 important evidence relevant to the origin of this unique meteorite.

84

2. Samples and analytical techniques

86   Two samples of NWA 7325 were available for bulk rock chemical analysis: a clean chip of the

87 interior of the meteorite (600 mg, fragment of the same slice used for the thick section), and a sample

88 of cutting dust recovered using distilled water during cutting of the stones by S. Ralew, the owner of

89 the meteorite. In addition, two low-Ti gabbroic pebbles from Vaca Muerta were selected for

90 comparison, from the mesosiderite samples studied previously by Greenwood et al. (2006).

91 Petrographic observations and quantitative chemical analyses of the main phases of the NWA 7325

92 achondrite were made on a polished thick section (1 cm^2) prepared from a slice obtained from S.

93 Ralew. Cameca SX100 electron microprobe analyses at Service Commun "Microsonde Ouest"

94 (Plouzané) were obtained at 15 kV accelerating voltage with a probe current of 12 nA. Minerals

95 [wollastonite (Si, Ca), orthoclase (K), albite (Na), apatite (P)], oxide [$MnTiO_3$ (Mn, Ti)], Al_2O_3 (Al),

96 Fe_2O_3 (Fe), Cr_2O_3 (Cr)], and one sulfide [FeS_2 (S)] were used for calibration. The raw data were

97 corrected with the 'PAP' software (Pouchou and Pichoir, 1985).

98

99   The Vaca Muerta samples and the NWA 7325 chip were totally powdered using a boron

100 carbide pestle and mortar. Major and trace element concentrations were determined respectively by

101 ICP-AES (inductively coupled plasma-atomic emission spectrometry) and ICP-MS (inductively

102 coupled plasma-mass spectrometry) at Université de Brest (IUEM, Plouzané) using the procedures

103 described by Barrat et al. (2012, 2014). The accuracy of major and trace element concentrations is

104 better than 5% (probably better than 3% for all the REEs) based on various standard and sample

105 duplicates.

106   Oxygen isotope analyses were carried out at the Open University using an infrared laser

107 fluorination system following the methods and procedures of Miller et al. (1999). Analyses were

108 undertaken using a powder prepared from the 600 mg internal sample of NWA 7325. Oxygen was

109 released from 2 mg aliquots by heating in the presence of BrF_5. After fluorination, the released oxygen

110 gas was purified by passing it through two cryogenic nitrogen traps and over a bed of heated KBr.

111 Oxygen gas was analysed using a MAT 253 dual inlet mass spectrometer. Interference at m/z=33 by

112 the NF_3 fragment ion NF^+ was monitored by performing scans for NF_2^+ on all samples run in this

113 study. In all cases NF_2 was either negligible or absent. Oxygen isotopic analyses are reported in

114 standard δ notation, where $\delta^{18}O$ has been calculated relative to VSMOW (Vienna Standard Mean

115 Ocean Water) as $\delta^{18}O = [(^{18}O/^{16}O_{sample})/(^{18}O/^{16}O_{VSMOW})-1] \times 1000$ (‰) and similarly for $\delta^{17}O$ using

116 the $^{17}O/^{16}O$ ratio. $\Delta^{17}O$, which represents the deviation from the terrestrial fractionation line, has been

117 calculated using a linearized format (Miller, 2002):

118 $$\Delta^{17}O = 1000 \ln(1 + \delta^{17}O/1000) - \lambda\ 1000 \ln(1 + \delta^{18}O/1000)$$

119 where $\lambda = 0.5247$, which was determined using 47 terrestrial whole-rock and mineral separate samples

120 (Miller et al., 1999; Miller, 2002). Recent levels of precision obtained on the Open University system,

121 as demonstrated by 39 analyses of our internal obsidian standard, were as follows: ±0.05‰ for $\delta^{17}O$;

122 ±0.09‰ for $\delta^{18}O$; ±0.02‰ for $\Delta^{17}O$ (2σ).

123   Carbon and nitrogen concentrations and isotopic analyses were obtained by the stepped

124 combustion technique using the multi-element analyzer system "Finesse" (Verchovsky et al., 1998,

125 2003). An aliquot (6.134 mg) of the internal sample of NWA 7325 was heated from 200 to 1400°C

126 with 100° increments. The released N and C in the form of N_2 and CO_2 were analyzed simultaneously

127   from the same aliquot. The isotope results are expressed in standard δ notation normalized to air for N

128   and to PDB for C.

129

3. Results and discussion

3.1. Petrography

132   NWA 7325 has been extensively described in a series of abstracts (Irving et al., 2013; Bischoff

133   et al., 2013; Goodrich et al., 2014; El Goresy et al., 2014). Our observations are in agreement with

134   these earlier studies, and are summarized here. NWA 7325 is a fine to medium grained gabbroic rock

135   with a grain size typically in the range of 0.5-1 mm (Fig. 1). It is unbrecciated, and consists of ~25-30

136   vol% diopsidic pyroxenes, ~15 vol% olivine grains surrounded or poikilitically enclosed by

137   plagioclase (~55-60 vol%), with accessory iron sulfides (1 vol%), and sparse ferrochromite, metal

138   grains and rare eskolaite associated with iron sulfide. El Goresy et al. (2014) report the occurrence of

139   Ca sulfates that they interpret as totally weathered grains of oldhamite. However, like the vast

140   majority of Saharan finds, NWA 7325 contains cracks filled with secondary carbonates. Rather than

141   being formed by the terrestrial alteration of oldhamite, we believe that the Ca sulfates in NWA 7325

142   are more likely to represent normal hot desert weathering products.

143   Major element compositions of the main phases are reported in Table 1. Coarse-grained

144   plagioclase is calcic (An_{85-93}), and contains traces of MgO (=0.13-0.45 wt%). Ca-pyroxene is

145   homogeneous and extremely magnesian ($En_{50.1-54.0}$ $Wo_{44.8-49.3}$ $Fs_{0.6-1.3}$, Mg/(Fe+Mg)= 0.975-0.983,

146   n=58). Olivine ($Fo_{97-97.3}$, n=51) is in equilibrium with pyroxene (e.g., Perkins and Vielzeuf, 1992). Fe-

147   sulfide is Cr-rich (Cr = 2.2-6 wt%) and contains lamellas of daubréelite.

148   Irving et al. (2013) noted that the plagioclase in NWA 7325 is finely mottled, and much less

149   birefringent than normal. It contains clusters of tiny grains of troilite and metal. They suggested that

150   the plagioclase has been totally melted, possibly as a result of shock, and reacted locally with olivine

151   to generate secondary diopside. This view has been challenged by Bischoff et al. (2013). They

152 observed plagioclase-rich veins and occasionally SiO_2-normative mesostases around mafic minerals

153 and within Ca-pyroxenes, which could have been formed upon shock. However, they pointed out that

154 olivine is only very weakly shocked (stage S2), suggesting that the shock pressure suffered by NWA

155 7325 was certainly not strong enough to melt it extensively.

156

3.2. Geochemistry

158 3.2.1. Major and trace element.

159   The major element composition of the cutting dust (Table 2) is very similar to the results

160 obtained at University of Alberta on a distinct sample of cutting dust (Irving et al., 2013). NWA 7325

161 is a basic rock, rich in MgO and Al_2O_3, and poor in Fe, Mn and alkalis (Na_2O = 0.6 wt%). Using the

162 average compositions of the main phases, it corresponds to an assemblage of about 55 wt%

163 plagioclase, 32 wt% pyroxene, 10 wt% olivine and traces of sulfides and secondary calcite, in

164 agreement with phase proportions estimated from the polished sections (see above).

165   Despite the similarity of their major element compositions, the trace element abundances of

166 the two cutting dust samples (this study and Irving et al., 2013) are different, and display some

167 significant discrepancies (Table 3 and Fig. 2 and 3). Both samples are poor in incompatible lithophile

168 elements (REEs except Eu < 2 x CI), light REE enriched (La_n/Sm_n = 1.95 – 2.90) with striking positive

169 Eu anomalies (Eu/Eu* = 16.1 – 35.2), but our sample contains respectively about 2x more light REEs,

170 and half the Th content reported by Irving et al. (2013). Furthermore, the Irving et al. (2013) sample

171 displays markedly high Nb and Hf abundances compared to our analysis. A number of possible

172 explanations might account for these differences: i) contamination during the cutting of the meteorite

173 by handling and by the saw blade, ii) different proportions of soil materials which were adhering to the

174 surface of the stones (see Fig. 1a), and, iii) different contributions from secondary phases (Fe-oxides,

175 carbonates and sulfates) along surfaces crossed by the saw blade. The low abundance of incompatible

176 lithophile elements (e.g., the light REEs, Th, U, Rb and Cs) makes them extremely sensitive to

177   terrestrial contamination, which could have taken place subsequent to its landing on the desert soil,

178   and/or by handling during the recovery and sample preparation. The soil of the strewnfield has not

179   been analyzed, but its Th and REE abundances are probably similar to those of the upper continental

180   crust average. Such a soil [as illustrated by the soil of Tatahouine (Barrat et al., 1999)] can contain ca.

181   100 times more La and Th than the cutting dust. A slight contamination by soil could be undetectable

182   with major elements, but have a huge impact on the abundances of many trace elements.

183   It is clear from the preceding section that the trace element composition of NWA 7325 should

184   be determined using material from clean interior chips. We prepared one such fraction using a

185   fragment weighing 600 mg. Its major element abundances deviate just slightly from the cutting dust

186   analyses, except for Fe which is three time less abundant in the chip than in the cutting dust.

187   Furthermore, the cutting dust contains much more Ni, Cu, Zn W and Pb than the interior chips, which

188   most likely result from contamination by the saw blade. We don't know exactly the composition of the

189   saw blade which was used here, but saw blades typically have diamond grit in them that are

190   electroplated to the steel blade with a Ni, Cu or Zn matrix. Therefore, most major element abundances

191   determined using cutting dust would appear to be representative of the whole rock, contrary to the

192   trace element contents which are not reliable and should be rejected (Tables 2 and 3).

193   Despite our effort to select a fragment that was as fresh as possible, terrestrial weathering

194   effects cannot be totally avoided. The mineralogical and chemical effects of hot desert weathering are

195   now relatively well understood, and have been previously documented in a range of meteorite types

196   (e.g., Barrat et al., 1999; 2004, 2010; Stelzner et al., 1999; Crozaz et al., 2003). Our interior chip is no

197   exception. As shown in Figures 2 and 3, it displays a high Ba abundance, a high U/Th ratio (= 1.1),

198   and a positive Ce anomaly (Ce/Ce* = 1.25). Such features have been repeatedly observed in weathered

199   Saharan finds, and it is not necessary to repeat here a discussion concerning their origin. Although

200   Saharan finds display often high Sr abundances, the positive Sr anomaly exhibited by NWA 7325 is

201   probably, like the Eu anomaly, a primary feature attributable to plagioclase.

202

203   NWA 7325 contains low but significant amounts of Ni (= 57 µg/g) and Co (=23 µg/g),

204   probably hosted by minute grains of metal (Table 3). It is poor in Zn, Cu and Pb. Its low lithophile

205   element abundances are well illustrated by the CI- normalized trace element patterns (Fig. 2 and 3).

206   Except for Sc, Ba, U, Sr and Eu, all the lithophile trace elements display concentration < 0.3 x CI.

207   Furthermore, the trace element patterns exhibit Cs, Rb, Zr, and Hf depletions. Contrary to the results

208   for the cutting dust, the interior fragment is light-REE depleted ($La_n/Sm_n = 0.70$), and displays large

209   positive Eu and Sr anomalies (Eu/Eu*= 65, Sr_n/Ce_n= 240).

210

211   3.2.2. Oxygen isotopes.

212   The bulk oxygen isotopic composition of NWA 7325 was determined in duplicate using the powder

213   made with the interior fragment. The average of the two analyses was: $\delta^{17}O$ =3.33 ± 0.09 ‰, $\delta^{18}O$ =

214   8.10 ± 0.18 ‰, $\Delta^{17}O$ = −0.91 ± 0.01 ‰ (errors ± 1σ). Our new analysis of NWA 7325 plots on the

215   CCAM line in Fig. 4, within the ureilite field. Three individual analyses of NWA 7325 by Irving et al.

216   (2013) have somewhat divergent compositions, with one plotting close to the result reported here.

217   Jabeen et al. (2014) give oxygen isotope analyses for plagioclase and pyroxene mineral separates from

218   NWA 7325 that are displaced from one another by approximately 2 ‰ along a mass fractionation line

219   (Fig. 4). The mean plagioclase analysis (n=4) of Jabeen et al. (2014) plots close to our bulk value for

220   NWA 7325. However, in view of the significant proportion of pyroxene in NWA 7325 (20-30 %,

221   section 3.1) the analyses of Jabeen suggest that, had they determined a bulk composition for the

222   meteorite, this would probably have been shifted to somewhat lower $\delta^{18}O$ values compared to our

223   analysis.

224

225   3.2.3. Carbon and nitrogen isotopes.

226   The results for C and N are presented in table 4 and Figure. 5. Carbon displays a bimodal

227   release with peaks in the range 200-400°C and 500-700°C. The low temperature peak is due to the

228   terrestrial contamination associated with both weathering during the residence of the meteorite on the

229   Earth's surface and laboratory handling and has a characteristic carbon isotopic composition ($\delta^{13}C$= -

230   27 to -29‰). The second peak seems to represent a terrestrial carbonate as indicated both by the

231   release temperature corresponding to that for decomposition of $CaCO_3$ and the isotopic composition

232   with $\delta^{13}C$ = -1 to 3‰. This interpretation is consistent with the petrographic data (see section 3.1).

233   Most of nitrogen is released at low T (200-700°C) and appears to predominantly reflect

234   terrestrial contamination. Isotopically it is relatively heavy and has a comparatively high (~0.1) C/N

235   ratio that also points to terrestrial organic contamination. The extension of the low T peak of nitrogen

236   to 700°C suggests that a part of the nitrogen is associated with the secondary carbonate.

237

238   ## 3.3. NWA 7325, a unique achondrite.

239

240   3.3.1. What is the parent body of NWA 7325?

241   As pointed out by Irving et al. (2013), various major element ratios (e.g., Al/Si and Mg/Si)

242   determined from NWA 7325 are within the range of values measured on Mercury's surface by remote

243   sensing observations (Weider et al., 2012). However, the suggestion that NWA 7325 may represent a

244   sample of Mercury's crust (Irving et al., 2013) has been challenged on the basis of dating evidence.

245   Amelin et al. (2013) obtained a Pb-isotopic age for NWA 7325 of 4562.5 ± 4.4 Ma. This very old age

246   was subsequently confirmed by Dunlap et al. (2014), who obtained an Al-Mg age of 4562.8 ± 0.3 Ma.

247   Both teams pointed out that NWA 7325 crystallized at the same time as angrites and some other

248   achondrites, and seems too old to be a sample of the differentiated crust of a planetary-sized body.

249   Therefore, a mercurian origin appears to be untenable, and instead it seems more likely that NWA

250   7325 originated from one of the planetesimals that formed during the first millions of years after the

251   formation of refractory inclusions.

252

253   Achondrites display a wide range of mineralogical compositions (e.g., Mittlefehldt et al., 1998).

254   Even if these rocks sampled a limited number of differentiated bodies, they formed under a variety of

conditions, and illustrate, at least partially, the diversity of primitive materials and conditions present in the early Solar System (i.e., highly reduced conditions for aubrites, a volatile-depleted body and more oxidized conditions for angrites, C-rich body with ureilites…). Despite this large mineralogical variability, achondrites displaying highly magnesian silicates and calcic plagioclases are exceptional. Only a unique mm-sized troctolitic clast found in the polymict ureilite Dar al Gani 319 displays phase compositions similar to NWA 7325 (plagioclase An_{87-89}, olivine Fo_{93}, Ikeda et al., 2000; Kita et al., 2004; Goodrich et al., 2014). Although the O-isotopic composition of NWA 7325 is in the range of the ureilites (Fig. 4), two important lines of evidence preclude these meteorites originating from the same body:

(i) Olivine cores in ureilites display a wide range of compositions which are correlated with the O isotopic composition of the bulk rocks (Clayton and Mayeda, 1996). If NWA 7325 formed from an ureilitic source, the latter would necessarily be among the most Mg-rich ureilites, which display the lowest $\Delta^{17}O$ values (< -2 ‰), inconsistent with the $\Delta^{17}O$ value of NWA 7325 (Fig. 6).

(ii) While ureilites display a restricted range of $\varepsilon^{54}Cr$ values close to -0.9 (e.g., Yamakawa et al., 2010), NWA 7325 has a distinct $\varepsilon^{54}Cr$ value of -0.55 ± 0.08, precluding this meteorite originating from the ureilite parent body (Sanborn et al., 2013).

Thus, NWA 7325 is a unique achondrite with distinctive geochemical and isotopic features. It certainly originated from a parent body unsampled by other achondrites. In Figure 7, we compare the Ga/Al, Zn/Al and Na/Al ratios in NWA 7325 (analyses from the interior chip, not the cutting dust samples) with other well-characterized achondrites. Unlike the martian achondrites, the ureilitic (ALM-A) and brachinitic (GRA-06) melts, NWA 7325 displays low Na/Al, Ga/Al and Zn/Al and plots near or in the fields of rocks from the Moon and Vesta, suggesting a volatile-depleted parent body. This inference is strengthened by the very low K, Rb and Cs abundances shown by the NWA 7325 chip (Table 3).

282   3.3.2. Petrology of NWA 7325

283   Discussing the petrology of a gabbroic rock that is the sole sample we have at present from an

284   unknown parent body is a challenging task. The huge positive Eu anomaly displayed by NWA 7325 is

285   unambiguously related to its abundant plagioclases and points to reduced conditions (e.g., Drake and

286   Weill, 1975), in agreement with the occurrence of traces of metal, Cr-rich sulfides. Indeed, the

287   valences of Cr, Ti, V in olivine and pyroxene determined by XANES spectroscopy suggest

288   crystallization conditions close to the Cr-CrO buffer (i.e. fO_2 close to IW-4, Sutton et al., 2014).

289

290   Gabbroic rocks displaying positive Eu anomalies are widely considered as cumulates. NWA

291   7325 is no exception (e.g., Irving et al., 2013), but we emphasize that this interpretation is not unique.

292   Significant positive Eu anomalies can be generated in non-cumulative basaltic rocks by partial

293   melting, for example during short duration reheating events (Yamaguchi et al., 2009; 2013). Larger

294   degrees of melting of a basaltic or gabbroic lithology can produce gabbroic restites displaying very

295   low incompatible trace element abundances and huge positive anomalies. Previous studies have

296   emphasized the complex thermal history of NWA 7325, and shown that its texture could be explained

297   by remelting (e.g., Bischoff et al., 2013). Thus, the possibility that NWA 7325 could be a restite merits

298   further consideration.

299

300   Partial melting has been previously proposed to explain the very low REE abundances and

301   very large Eu anomalies displayed by some gabbroic pebbles found in mesosiderites (e.g., Rubin and

302   Mittlefehldt, 1992). We analyzed for comparison two such pebbles from Vaca Muerta (Table 2 and

303   Figures 2 and 3). These meteorites are finds from the Atacama Desert. They display some anomalies

304   that are certainly the result of terrestrial weathering, and that do not require further consideration here,

305   i.e. positive Ce anomalies, sometimes high U/Th ratios and high Pb abundances, etc… Interestingly,

306   these two pebbles display at first glance the same level of incompatible trace element concentrations

307   and the same large Sr and Eu anomalies as NWA 7325. However, their REE patterns display marked

308   heavy-REE enrichments (Gd_n/Lu_n = 0.14-0.43) which are well explained by the loss of a partial melt

309   (e.g., Yamaguchi et al., 2009). The REE pattern of the NWA 7325 chip does not exhibit such an

310   enrichment ($Gd_n/Lu_n = 2.92$). We conclude that NWA 7325 is probably not restitic, although we note

311   that this inference is model dependent (i.e., composition of the melted lithology).

312

313   If NWA 7325 is a cumulate, what can we infer about the composition of its parental melt

314   based on its petrography and major and trace element abundances? It was certainly "basaltic", not

315   SiO_2-saturated (crystallization of olivine), and Ca-rich (diopsidic pyroxene and calcic plagioclase). It

316   was certainly Na-poor (calcic plagioclase) and of course displayed a very low FeO/MgO in order to

317   explain the very high Mg/(Fe+Mg) ratios of the olivines and pyroxenes. Moreover, NWA 7325

318   displays very low abundances of incompatible trace elements. Its parental melt was certainly very poor

319   in these elements. While it is not possible to precisely constrain its trace element abundances, some

320   very simple assumptions allow us to qualitatively evaluate some of its features. Partition coefficients

321   for Yb or Lu in diopside are about 10 times larger than those for plagioclase or olivine (e.g., McKay et

322   al., 1989; Schosnig and Hoffer, 1998). Consequently, in a cumulate like NWA 7325, made essentially

323   of plagioclase, diopsidic pyroxene and olivine, the pyroxene controls the budget of heavy REEs.

324   Assuming that the NWA 7325 chip contained about 33 wt% pyroxene, the Yb or Lu concentrations in

325   this mineral are probably ≈ 0.15 x CI abundances. Partition coefficients of Yb for diopside at low

326   pressure range from 0.1 and 0.6 (Schosnig and Hoffer, 1998, and references therein) suggesting Yb or

327   Lu abundances in the range of 0.25 to 1.5 x CI abundances only in the parental melt. Furthermore, the

328   shape of its REE pattern was probably not chondritic. Again, since clinopyroxene controls the heavy

329   REE abundances in NWA 7325, the Gd-Lu part of the REE pattern is chiefly controlled by its partition

330   coefficients and the $(Gd/Lu)_n$ of the parental melt. Because $(D_{Gd}/D_{Lu})_{cpx}$ is ≈ 1 (e.g., Schosnig and

331   Hoffer, 1998), $(Gd/Lu)_n$ ratios close to 1 are expected for pure cumulates formed from a chondritic

332   melt. This inference remains valid even if the cumulates contain some trapped melt. As a consequence,

333   the high $(Gd/Lu)_n$ ratio (=2.92) displayed by the NWA 7325 chip is inconsistent with a parental melt

334   displaying a flat REE pattern. The parental melt to NWA 7325 must therefore have had a fractionated

335   REE pattern with $(Gd/Lu)_n$ ratio > 1, and probably ≈ 3. Similar lines of reasoning are possible for Eu.

336   Partition coefficients for Eu in plagioclase are much larger than those in pyroxene or olivine (e.g.,

337   McKay et al., 1989; Schosnig and Hoffer, 1998). Therefore, the budget of Eu in the rock is strongly

338   controlled by plagioclase. Assuming that the NWA 7325 chip contained about 53 wt% plagioclase, the

339   Eu concentration in this phase is ≈ 16 x CI abundance. Partition coefficients for Eu in plagioclase are

340   not only dependent on the composition of the melt but are also strongly sensitive to the oxygen

341   fugacity (e.g., McKay, 1989). For the purpose of calculation, partition coefficients for Eu in calcic

342   plagioclase at low fO_2 for a basaltic melt are assumed to range from 0.7 to 1.1 as suggested by McKay

343   (1989), and in agreement with the recent experimental results obtained by Rapp et al. (2015). The Eu

344   concentration of the parental melt was probably in the range of 14 to 23 x CI abundances. Even if we

345   take into account the enrichment in middle REEs of the parental melt (i.e., the $(Gd/Yb)_n$ or the

346    $(Gd/Lu)_n$ ratios), its level of concentration of Eu is very high compared to the heavy-REEs. It comes as

347   an unavoidable conclusion that the parental melt of NWA 7325 certainly displayed a very large

348   positive Eu anomaly ($Eu_n/Yb_n > 10$, probably $Eu_n/Gd_n > 3$) that is difficult to estimate accurately.

349   A melt with such a large positive Eu is very unlikely to be the direct product of the early

350   magmatic activity on a planetesimal. On the other hand, gabbros formed in reduced conditions can

351   display low incompatible trace element abundances and large positive Eu, as exemplified by the

352   cumulate eucrites. Total melting of such rocks could produce melts with these features. It is tempting

353   to propose that NWA 7325 is a cumulate derived from the crystallization of such a melt, with the

354   melting of its protolith possibly produced by an energetic impact.

355

356   Recent data for NWA 7325 allow us to further evaluate this hypothesis. Highly Siderophile

357   Elements (HSEs) are sensitive tracers of chondritic contributions in impact melts and impactites. Two

358   samples were analyzed by Archer et al. (2015). Their abundances differ from one another by almost

359   one order of magnitude, and demonstrate that the HSE carriers are heterogeneously distributed in the

360   bulk rock. The sample displaying the highest abundances shows a chondritic distribution of HFEs, in

361   agreement with a possible projectile contribution (it contains about 0.9 ng/g Ir, suggesting the addition

362   of ≈0.2 wt% of chondritic material). Archer et al. (2015) suggested that this chondritic signature was

363   introduced into the rock after crystallization during late-stage impacts. Because NWA 7325 is

364   unbrecciated, this explanation is unlikely. Alternatively, a chondritic component could have been

365   introduced into the NWA 7325 parental melt during its crystallization. One possibility is that NWA

366 7325 became contaminated through interaction with regolith material. The parental melt could have

367 inefficiently assimilated regolith containing chondritic debris. However, as pointed out by Archer et al.

368 (2015), an assimilation process that only partially affected the rock, is difficult to envisage. Instead, a

369 heterogeneously distributed chondritic signature in NWA 7325 is best explained if this meteorite was

370 derived from the crystallization of an impact melt.

371 Moreover, the systematics of ^{26}Al-^{26}Mg further strengthens the hypothesis that NWA 7325

372 formed by impact-melting of gabbroic material. The Al-Mg internal isochron obtained previously by

373 Dunlap et al. (2014) for NWA 7325 has a well-resolved positive intercept ($\delta^{26}Mg_0*$) of 0.095 ± 0.011

374 ‰, and lies well above the bulk chondritic value (Al/Mg ≈ 0.1 and $\delta^{26}Mg* \approx 0$ ‰). As noted by

375 Dunlap et al. (2014), this high $\delta^{26}Mg_0*$ could imply a non-chondritic initial composition for the

376 parental body. Alternatively, the source material for this achondrite may have evolved with a highly

377 superchondritic Al/Mg ratio early in the history of the solar system prior to the heating event that

378 formed the melt that was parental to NWA 7325. Gabbros and plagioclase-rich cumulates are Al-rich

379 compared to chondrites, and exhibit highly superchondritic Al/Mg ratios. The impact-melting

380 hypothesis of this kind of rock offers a straightforward explanation for the distinctly high $\delta^{26}Mg_0*$ of

381 NWA 7325 (Fig. 8). Moreover, assuming that the parental melt of NWA 7325 formed by impact

382 melting of a gabbroic target 4.5628 Ga ago, we can place some constraints on the formation age of its

383 protolith. Unfortunately, the ^{27}Al/^{24}Mg ratio of the parental melt of NWA 7325 is not known. Because

384 NWA 7325 is a plagioclase rich cumulate, its parental melt displayed probably a lower Al abundance

385 than the whole rock, but it is not possible to assess neither its Mg concentration nor its Al/Mg ratio. In

386 the case of eucrites, the Al/Mg ratios of cumulate and basaltic eucrites are similar. Although these

387 rocks are probably not perfect analogs of NWA 7325, we can reasonably propose that the situation

388 was comparable for NWA 7325 and its parental melt. For the purpose of calculation, we used the

389 whole rock ^{27}Al/^{24}Mg ratio (= 1.56) and we obtained an intercept with the solar system growth curve at

390 about 4566 Ma. A lower Al/Mg ratio would point to an older model age, and conversely younger

391 model ages are obtained with higher Al/Mg ratios, but variations of 25 % around the Al/Mg ratio of

392 the whole rock do not alter this estimation (Fig. 9). Although only indicative, our calculations show

393 that remelting of a very old gabbroic lithology can perfectly explain the high $\delta^{26}Mg*_0$ of NWA 7325.

394 Thus, NWA 7325 provides evidence of one of the earliest crusts on a differentiated body so far

395 studied. We note that the NWA 7325 protolith could be practically contemporaneous to Asuka

396 881394, which formed 4566.5 ± 0.2 Ma ago on a distinct parent body (Wadhwa et al., 2009).

397

398 ## 4. Conclusions

399   Two important conclusions emerge from this study. The first one is methodological. While it

400 is often very difficult to obtain representative samples of rare meteorites, the use of cutting dust should

401 be avoided, at least for the trace element analyses. Secondly, our data confirm that NWA 7325 is a

402 new type of achondrite that originated from a parent body not previously sampled by the other

403 meteorites. Despite their similar oxygen isotope compositions, a number of lines of evidence preclude

404 a relationship between NWA 7325 and the ureilites. NWA 7325 is a gabbroic rock that displays

405 distinct phase compositions, notably highly magnesian pyroxenes and olivine. Its chemical

406 composition suggests that it formed from an unusual melt characterized by very low incompatible

407 trace element abundances and a very large positive Eu anomaly. We propose that this melt formed by

408 the remelting of an ancient gabbroic lithology, possibly upon impact, in agreement with the HSE

409 abundances, and the systematics of ^{26}Al-^{26}Mg. Based on recent dating, the crustal material that was

410 parental to NWA 7325 must have been older than 4562.8 Ma. Thus, NWA 7325 provides evidence of

411 one of the earliest crusts on a differentiated body so far studied and indicates how such materials were

412 rapidly recycled.

422

References

423

424 Amelin Y., Koefoed P., Iizuka T., Irving A.J. (2013) U-Pb age of ungrouped achondrite NWA 7325. *76th Annual*
425   *Meteoritical Society Meeting*, abstract # 5165.

426 Archer G.J., Walker R.J., and Irving A.J. (2015) Highly siderophile element and 187Re-187Os isotopic
427   systematics of ungrouped achondrite Northwest Africa 7325. *46th Lunar Planet. Sci. Conf.*, abstract # 1987.

428 Barrat J.A., Gillet Ph., Lesourd M., Blichert-Toft J. and Poupeau G.R. (1999) The Tatahouine diogenite:
429   mineralogical and chemical effects of 63 years of terrestrial residence. *Meteoritics Planet. Sci.* **34**, 91-97.

430 Barrat J.A., Jambon A., Bohn M., Blichert-Toft J., Sautter V., Göpel C., Gillet Ph., Boudouma O., and Keller F.
431   (2003) Petrology and geochemistry of the unbrecciatted achondrite North West Africa 1240 (NWA 1240):
432   an HED parent body impact melt. *Geochim. Cosmochim. Acta* **67**, 3959-3970.

433 Barrat J.A., Yamaguchi A., Zanda B., Bollinger C., Bohn M. (2010) Relative chronology of crust formation on
434   asteroid 4-Vesta: Insights from the geochemistry of diogenites. *Geochim. Cosmochim. Acta.* **74**, 6218-6231.

435 Barrat J.A., Zanda B., Moynier F., Bollinger C., Liorzou C., and Bayon G. (2012) Geochemistry of CI
436   chondrites: Major and trace elements, and Cu and Zn isotopes. *Geochim. Cosmochim. Acta* **83**, 79-92.

437 Barrat J.A., Zanda B., Jambon A., Bollinger C. (2014) The lithophile trace elements in enstatite chondrites.
438   *Geochim. Cosmochim. Acta.* **128**, 71-94.
439
440 Bischoff A., Ward D., Weber I., Morlok A., Hiesinger H., Helbert J. (2013) NWA 7325 – not a typical olivine
441   gabbro, but a rock experienced fast cooling after a second (partial) melting. *European Planet. Sci. Congress*
442   **8**, EPSC2013-427 (abstract).
443
444 Bischoff A., Horstmann M., Barrat J.A., Chaussidon M., Pack A., Herwartz D., Ward D., Vollmer C., Decker S.
445   (2014) trachyandesitic volcanism in the early Solar System. *PNAS* **111**, 35, 12689-12692.
446
447 Clayton R.N., Mayeda T.K. (1996) Oxygen isotope studies of achondrites. *Geochim. Cosmochim. Acta* **60**, 1999-
448   2017.
449
450 Clayton R.N., Mayeda T.K. (1999) Oxygen isotope studies of carbonaceous chondrites. *Geochim. Cosmochim.*
451   *Acta* **63**, 2089-2104.
452
453 Crozaz G., Floss C., and Wadhwa M. (2003). Chemical alteration and REE mobilization in meteorites from hot
454   and cold deserts. *Geochim. Cosmochim. Acta* **67**, 4727-4741.
455
456 Day J.M.D. *et al.* (2012) Origin of felsic achondrites Graves Nunataks 06128 and 06129, and ultramafic
457   brachinites and brachinite-like achondrites by partial melting of volatile-rich primitive parent bodies.
458   *Geochim. Cosmochim. Acta* **81**, 94–128.
459
460 Downes, H., Mittlefehldt, D.W., Kita, N.T., Valley, J.W. (2008) Evidence from polymict ureilite meteorites for a
461   disrupted and re-accreted single ureilite parent asteroid gardened by several distinct impactors. *Geochim*
462   *Cosmochim Acta* **72**, 4825–4844.
463
464 Downes, H., Abernethy, F. A. J., Smith, C. L., Ross, A. J., Verchovsky, A. B., Grady, M. M., Jenniskens, P., and
465   Shaddad, M, H. (2015) Isotopic composition of carbon and nitrogen in ureilitic fragments of the Almahata
466   Sitta meteorite, *Meteoritics Planet. Sci.* **50**, 255-272.
467
468 Drake M. J. and Weill D. F. (1975) Partition of Sr, Ba, Eu^{2+}, Eu^{3+}, and other REE between plagioclase feldspar
469   and magmatic liquid: An experimental study. *Geochim. Cosmochim. Acta* **39**, 689–712.
470
471 Dunlap D.R., Wadhwa M., Romaneillo S.R. (2014) ^{26}Al-^{26}Mg systematics in the unusual ungrouped achondrite
472   NWA 7325 and the eucrite Juvinas. 45th Lunar Planet. Sci. Conf., abstract # 2186.

473

474 El Goresy A., Nakamura T., Miyahara M., Ohtani E., Gillet P., Jogo K., Yamanobe M., Ishida H. (2014) The
475   unique differentiated meteorite NWA 7325: highly reduced, stark affinities to E-chondrites and unknown
476   parental planet. *77th annual Meteoritical Society Meeting*, abstract # 5028.
477

478 Goodrich, C. A., Wlotzka, F., Ross, D. K. and Bartoschewitz, R. (2006) NWA 1500: plagioclase-bearing
479   monomict ureilite or ungrouped achondrite? *Meteoritics Planet. Sci.* **41**, 925–952.
480

481 Goodrich C.A., Harlow G.E., Van Orman J.A., Sutton S.R., Jercinovic M.J., Mikouchi T. (2014) Petrology of
482   chromite in ureilites: Deconvolution of primary oxidation states and secondary reduction processes.
483   *Geochim. Cosmochim. Acta* **135**, 126-169.

484 Goodrich C.A., Kita N.T., Nakashima D. (2014) Petrology of the NWA 7325 ungrouped achondrite – Meteorite
485   from Mercury, the Ureilite Parent Body, or a previously unsampled asteroid? *45th Lunar Planet. Sci. Conf.*,
486   abstract # 1246.
487

488 Greenwood R.C., Franchi I.A., Jambon A., Barrat J.A., Burbine T.H. (2006) Oxygen isotope variation in stony-
489   iron meteorites. *Science* **313**, 1763-1765.

490 Greenwood R.C., Barrat J.A., Yamaguchi A., Franchi I.A., Scott E.R.D., Bottke W.F., Gibson J.M. (2014) The
491   oxygen isotope composition of diogenites: Evidence for early global melting on a single, compositionally
492   diverse, HED parent body. *Earth Planet. Sci. Lett.* **390**, 165-174.
493

494 Greenwood R.C., Franchi I.A., Gibson J.M., Benedix G.K. (2012) Oxygen isotope variation in primitive
495   achondrites: The influence of primordial, asteroidal and terrestrial processes. *Geochim. Cosmochim. Acta*
496   **94**, 146–163.
497

498 Irving A.J., Kuehner S.M., Bunch T.E., Ziegler K., Chen G., Herd C.D.K., Conrey R.M., Ralew S. (2013)
499   Ungrouped mafic achondrite Northwest Africa 7325: a reduced, iron poor cumulate olivine gabbro from a
500   differentiated planetary body. *44th Lunar Planet. Sci. Conf.*, abstract #2164.
501

502 Jabeen I., Ali A., Banerjee N.R., Osinski G.R., Ralew S., DeBoer S. (2014) Oxygen isotope compositions of
503   mineral separates from NWA 7325 suggest a planetary (Mercury?) origin. *45th Lunar Planet. Sci. Conf.*,
504   abstract # 2215.
505

506 Keil K. (2010) Enstatite achondrite meteorites (aubrites) and the histories of their asteroidal parent bodies.
507   *Chemie der Erde-Geochemistry* **70**, 295–317.
508

509 Keil K. (2012) Angrites, a small but diverse suite of ancient, silica-undersaturated volcanic-plutonic mafic
510   meteorites, and the history of their parent asteroid. *Chemie der Erde* **72**, 191-218.
511

512 Keil, K. (2014) Brachinite meteorites: Partial melt residues from an FeO-rich asteroid. *Chemie der Erde* **74**, 311-
513   329.
514

515 Kita N.T., Sanborn M.E., Yin Q.Z., Goodrich C.A. (2014) The NWA 7325 ungrouped achondrite – Possible link
516   to ureilite? Oxygen and chromium isotopes and trace element abundances. 45th Lunar Planet. Sci. Conf.,
517   abstract # 1455.
518

519 Love S.G., Keil K. (1995) Recognizing mercurian meteorites. *Meteoritics* **30**, 269-278.
520

521 McKay G. A. (1989) Partitioning of rare earth elements between major silicate minerals and basaltic melts. *Rev.*
522   *Mineral. Geochem.* **21**, 45–77.
523

524 Miller M.F. (2002) Isotopic fractionation and the quantification of ^{17}O anomalies in the oxygen three isotopes
525   system: an appraisal and geochemical significance. *Geochim. Cosmochim. Acta* **66**, 1881-1889.
526

527 Miller M.F., Franchi I.A., Sexton A.S., Pillinger C.T. (1999) High precision ^{17}O isotope measurements of
528   oxygen from silicates and other oxides: Method and applications. *Rapid Commun. Mass Spectrom.* **13**,1211-
529   1217.
530

Mittlefehldt, D.W., McCoy, T.J., Goodrich, C.A., Kracher, A. (1998) Non-chondritic meteorites from asteroidal bodies. In: Papike, J.J. (Ed.), Planetary Materials. Miner-alogical Society of America, Washington, DC, 195 pp.

Perkins D., Vielzeuf D. (1992) Experimental investigation of Fe-Mg distribution between olivine and clinopyroxene: Implications for mixing properties of Fe-Mg in clinopyroxene and garnet-clinopyroxene thermometry. *American Mineralogist* **77**, 774-783.

Pouchou, J.L., Pichoir, F. (1985) 'PAP' procedure for improved quantitative microanalysis. *Microbeam Anal.* **54**, 104–106.

Rapp J.F., Lapen T.J., Draper D.S. (2015) REE partitioning in lunar minerals. 46th Lunar Planet. Sci. Conf., abstract # 2878.

Rubin A.E., Mittlefehldt D.W. (2012) Classification of mafic clasts from mesosiderites: implications for endogenous igneous processes. *Geochimica Cosmochimica Acta* **56**, 827-840.

Sanborn M.E., Yamakawa A., Yin Q.Z., Irving A.J., Amelin Y. (2013) Chromium isotopic studies of ungrouped achondrites NWA 7325, NWA 2976, and NWA 6704. *76th Annual Meteoritical Society Meeting*, abstract # 5220.

Schosnig M., Hoffer E. (1998) Compositional dependence of REE partitioning between diopside and melt at 1 atmosphere. *Contrib. Mineral. Petrol.* **133**, 205-216.

Singletary, S. J. and Grove, T. L. (2003) Early petrologic processes on the ureilite parent body. *Meteorit. Planet. Sci.* **38**, 95–108.

Stelzner T., Heide K., Bischoff A., Weber A., Weber D., Scherer P., Schukz L., Happel M., Schrön W., Neupert U., Michel R., Clayton R. N., Mayeda T. K., Bonani G., Haidas I., Ivy-Ochs S., and Suter M. 1999. In interdisciplinary study of weathering effects in ordinary chondrites from the Acfer region Algeria. *Meteoritics Planet. Sci.* **34**, 787–794.

Sutton S.R., Wirick S., Goodrich C.A. (2014) Ungrouped achondrite NWA 7325: titanium, vanadium and chromium XANES of mafic silicates record highly-reduced origin. **45th** *Lunar Planet. Sci. Conf.*, abstract # 1275.

Verchovsky, A.B., Fisenko, A.V., Semjonova, L.F., Wright, I.P., Lee, M.R., Pillinger, C.T. (1998) C, N, and noble gas isotopes in grain size separates of presolar diamonds from Efremovka. Science 281, 1165-1168.

Verchovsky, A.B., Sephton, M.A., Wright, I.P., Pillinger, C.T. (2002) Separation of planetary noble gas carrier from bulk carbon in enstatite chondrites during stepped combustion. *Earth Planetary Science Letters* **199**, 243-255.

Wadhwa M., Hamelin Y., Bogdanovski O., Shukolyukov A., Lugmair G.W., Janney P. (2009) Ancient relative and absolute ages for a basaltic meteorite: Implications for timescale of planetesimal accretion and differentiation. *Geochim. Cosmochim. Acta* **73**, 5189-5201.

Warren P.H., Rubin A.E., Isa J., Brittenham S., Ahn I., Choi B.G. (2013) Northwest Africa 6693: a new type of FeO-rich, low-Δ^{17}O, poikilitic cumulate achondrite. *Geochim. Cosmochim. Acta* **107**, 135-154.

Weber I., Morlok A., Bischoff A., Hiesinger H., Helbert J. (2014) Mineralogical and spectroscopic studies on NWA 7325 as an analogue sample for rocks from Mercury. 45th Lunar Planet. Sci. Conf., abstract # 1323.

Weider Z.S., Nittler L.R., Starr R.D., McCoy T.J., Stockstill-Cahill K.R., Byrne P.K., Denevi B.W., Head J.W., Salomon S.C. (2012) Chemical heterogeneity on Mercury's surface revealed by the MESSENGER X-Ray Spectrometer. *J. Geophys. Res.* **117**, E00L05, doi: 10.1029/2012JE004153.

Yamaguchi A., Clayton R. N., Mayeda T. K., Ebihara M., Oura Y., Miura Y. N., Haramura H., Misawa K., Kojima H., and Nagao K. (2002) A new source of basaltic meteorites inferred from Northwest Africa 011. *Science* **296,** 334–336.

588
589 Yamaguchi A., Barrat J.A., Greenwood R.C., Shirai N., Okamoto C., Setoyanagi T., Ebihara M., Franchi I.A.,
590   Bohn M. (2009) Crustal partial melting on Vesta : evidence from highly metamorphosed eucrites. *Geochim.*
591   *Cosmochim. Acta* **73**, 7262-7182.
592
593 Yamaguchi A., Mikouchi T., Ito M., Shirai N., Barrat J.A., Messenger S., Ebihara M. (2013) Experimental
594   evidence of fast transport of trace elements in planetary crusts by high temperature metamorphism. *Earth*
595   *Planet. Sci. Lett*. **368**, 101-109.
596
597 Yamakawa A., Yamashita K., Makishima A., Nakamura E. (2010) Chromium isotope systematics of
598   achondrites: Chronology and isotopic heterogeneity of the inner solar system bodies. *Astrophys J.* **720**, 150–
599   154.

600
601
602
603
604

605 Table 1. Average compositions of main phases in NWA 7325 (in wt%).

	n	SiO_2	TiO_2	Al_2O_3	Cr_2O_3	FeO	MnO	MgO	CaO	Na_2O	K_2O	Total	endmembers
plagio.	71	45.25	< 0.03	34.14	< 0.03	0.07	< 0.03	0.29	18.11	1.18	< 0.03	99.07	$An_{89.4}\,Ab_{10.5}$
pyrox.	58	52.68	0.04	2.93	1.03	0.73	0.05	18.88	22.54	0.16	< 0.03	99.04	$En_{53.2}\,Wo_{45.6}\,Fs_{1.2}$
olivine	51	42.25	< 0.03	0.04	0.37	2.81	0.07	54.38	0.35	< 0.03	< 0.03	100.25	$Fo_{97.2}$

	Si	Ti	Al	Cr	Fe	Mn	Mg	Ca	Na	S	Total
sulfide	0.04	< 0.03	< 0.03	3.57	59.62	< 0.03	0.01	0.15	< 0.03	37.64	101.19

(sulfide: 13)

606

607

608

609 Table 2. Major element compositions of NWA 7325 and two low-Ti Vaca Muerta pebbles (in wt%, *:
610   SiO_2 calculated by difference). Data given by Irving et al. (2013) obtained at University of
611   Alberta, are shown for comparison.

612

	NWA 7325			Vaca Muerta	
	cutting dust		chip	VM3	VM4
Lab.	U. Alberta	Brest	Brest	Brest	Brest
SiO_2	47.09	48.04	(46.4*)	(50.0*)	(46.0*)
TiO_2	0.01	0.05	0.03	0.04	0.06
Al_2O_3	18.6	18.91	17.83	9.65	13.14
Cr_2O_3	0.40	0.44	0.54	0.36	0.35
FeO	1.57	1.87	0.57	19.72	19.74
MnO	0.03	0.04	0.03	0.60	0.58
MgO	12.13	12.18	13.84	10.84	9.69
CaO	17.94	18.37	20.15	8.30	10.05
Na_2O	0.60	0.65	0.63	0.17	0.27
K_2O	0.01	0.03	<0.01	0.03	0.02
P_2O_5	0.02	0.03	0.04	0.30	0.12
total	98.40	100.61	100.00*	100.00*	100.00*

613

614

615   Table 3. Trace element abundances in NWA 7325 and in two low-Ti Vaca Muerta pebbles (in µg/g).

| Lab. | NWA 7325 | | | Vaca Muerta | |
	cutting U. Alberta	dust Brest	chip Brest	VM3 Brest	VM4 Brest
Li	0.53	0.93	0.32	3.86	4.22
Be		0.028	0.002	0.010	0.021
P_2O_5 wt%	0.02	0.043	0.024		
K	83	281	23		
Sc		19.64	24.18	29.38	25.41
Ti		239	106	215	361
V		190	249	83.8	85.3
Mn	230	260	254	4246	4097
Co		21.7	23.5	53.1	38.0
Ni	78	164	57	1278	716
Cu		264	6.76	13.6	14.2
Zn		330	5.23	1.97	1.01
Ga		8.32	8.65	1.36	1.58
Rb	0.37	0.86	0.055	0.14	0.18
Sr	198	195	189	37.0	54.9
Y		0.566	0.152	0.064	0.210
Zr	1.3	1.68	0.080	0.98	0.18
Nb	2.5	0.208	0.026	0.12	0.12
Cs		0.043	0.004	0.010	0.009
Ba	61	67.92	14.92	2.48	1.59
La	0.15	0.421	0.0188	0.0585	0.101
Ce	0.34	0.927	0.0612	0.179	0.279
Pr		0.109	0.00755	0.0201	0.0328
Nd	0.16	0.430	0.0413	0.0801	0.127
Sm	0.05	0.0944	0.0175	0.0165	0.0185
Eu	0.58	0.532	0.499	0.176	0.286
Gd	0.05	0.107	0.0308	0.0124	0.0145
Tb		0.0165	0.00484	0.00192	0.00286
Dy		0.0978	0.0302	0.0117	0.0243
Ho		0.0191	0.00573	0.00272	0.00764
Er		0.0521	0.0133	0.00855	0.0315
Yb		0.0452	0.00985	0.0174	0.0658
Lu		0.00635	0.00126	0.00348	0.0125
Hf	0.44	0.049	0.00340	0.0165	0.0035
Ta		0.0170	0.0009	0.011	0.009
W		0.112	<0.001	0.020	<0.001
Pb		3.91	0.027	2.64	0.19
Th	0.27	0.112	0.00901	0.00661	0.0107
U		0.0409	0.00987	0.00591	0.00295

616

617 Table 4. Nitrogen and Carbon isotope results. The sample weight was 6.143 mg.
618
619

T (°C)	C (ng)	δ^{13}C (‰)	±	N (ng)	δ^{15}N (‰)	±
200	151	-28.8	0.1	1.82	-4.7	1.4
300	1081	-28.7	0.2	117.7	10.6	0.2
400	533	-27.5	0.2	28.31	4.8	0.2
500	479	-22.2	0.2	23.63	5.5	0.3
600	2241	1.2	0.2	15.53	2.6	0.3
700	2542	3.0	0.2	13.84	3.0	0.4
800	71	-12.6	0.1	3.35	1.1	0.9
900	18	-14.4	0.2	2.17	11.9	1.3
1000	43	-13.1	0.5	0.86	16.5	2.1
1100	8	-16.9	0.2	0.52	-3.1	3.5
1200	15	-22.7	0.2	0.53	11.0	4.1
1300	9	-23.9	0.1	0.42	11.3	5.2
1400	39	-24.9	0.2	0.89	42.5	2.4
	7237	-7.4		210.6	8.0	

620
621
622

623

624

625
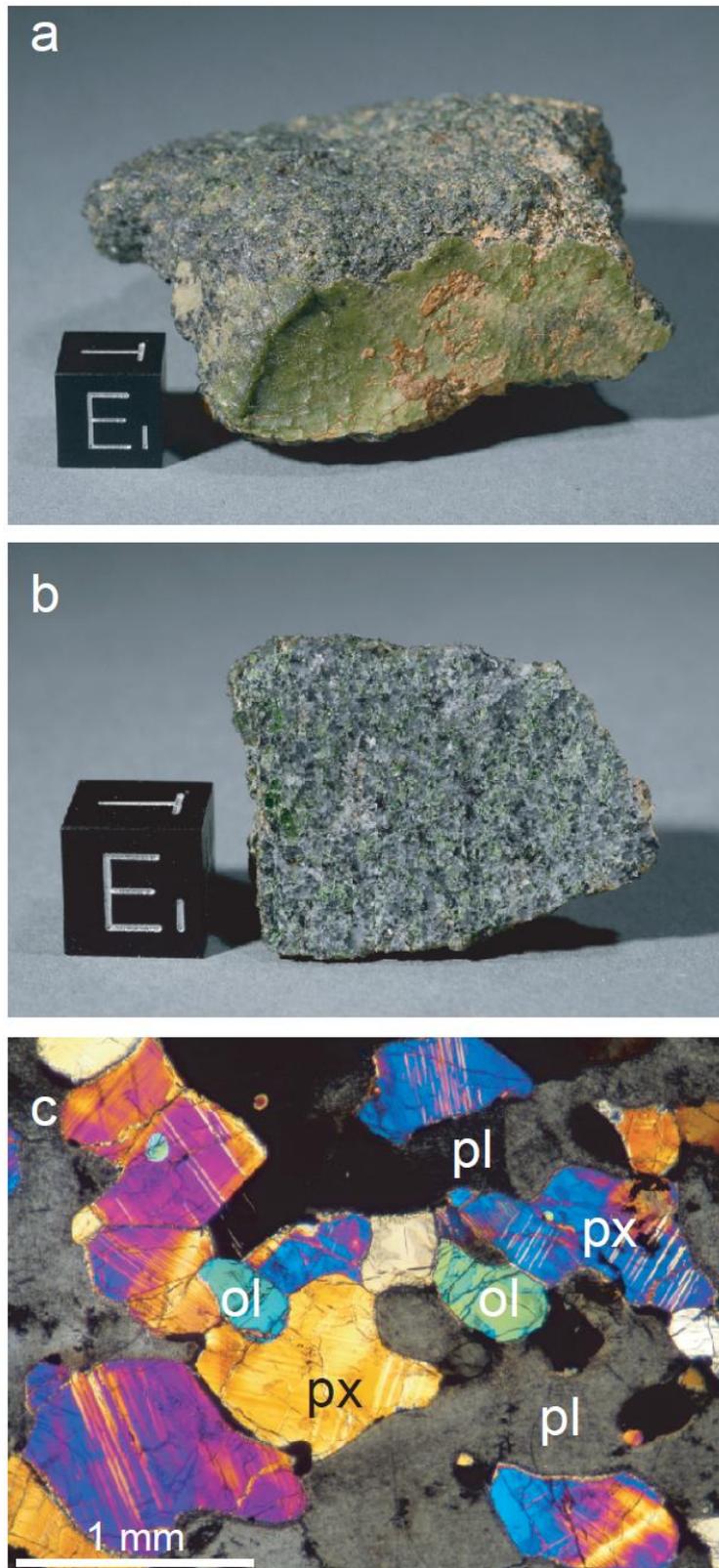
Figure 1. a: one of the largest NWA 7325 stones; notice the distinctive green fusion crust and the soil

materials adhering to the stone; the size of the cube is 1 cm; b: slice of NWA 7325 showing its

628   unbrecciated structure; c: crossed polarized light image of a thin section showing the gabbroic texture.

629   (Pictures a and b, courtesy of Stefan Ralew, picture c, courtesy of John Kashuba).

630

631

632
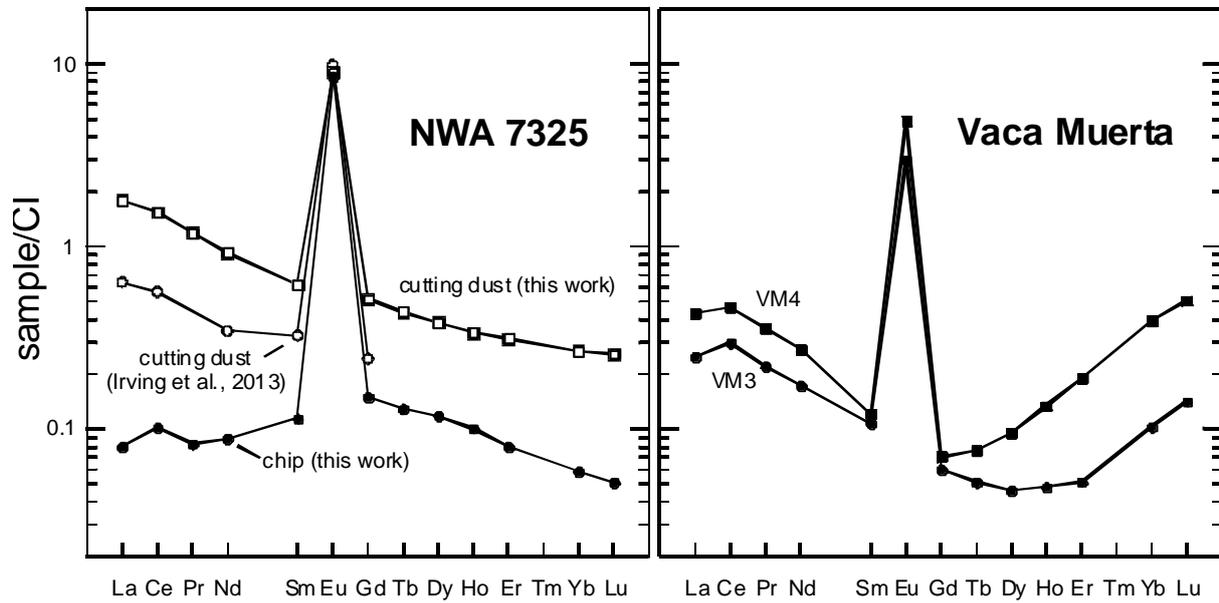
633   Figure 2. REE patterns of NWA 7325 and two low-Ti gabbros from the Vaca Muerta mesosiderite.

634   The reference CI chondrite is from Barrat et al. (2012).

635

636

637

638
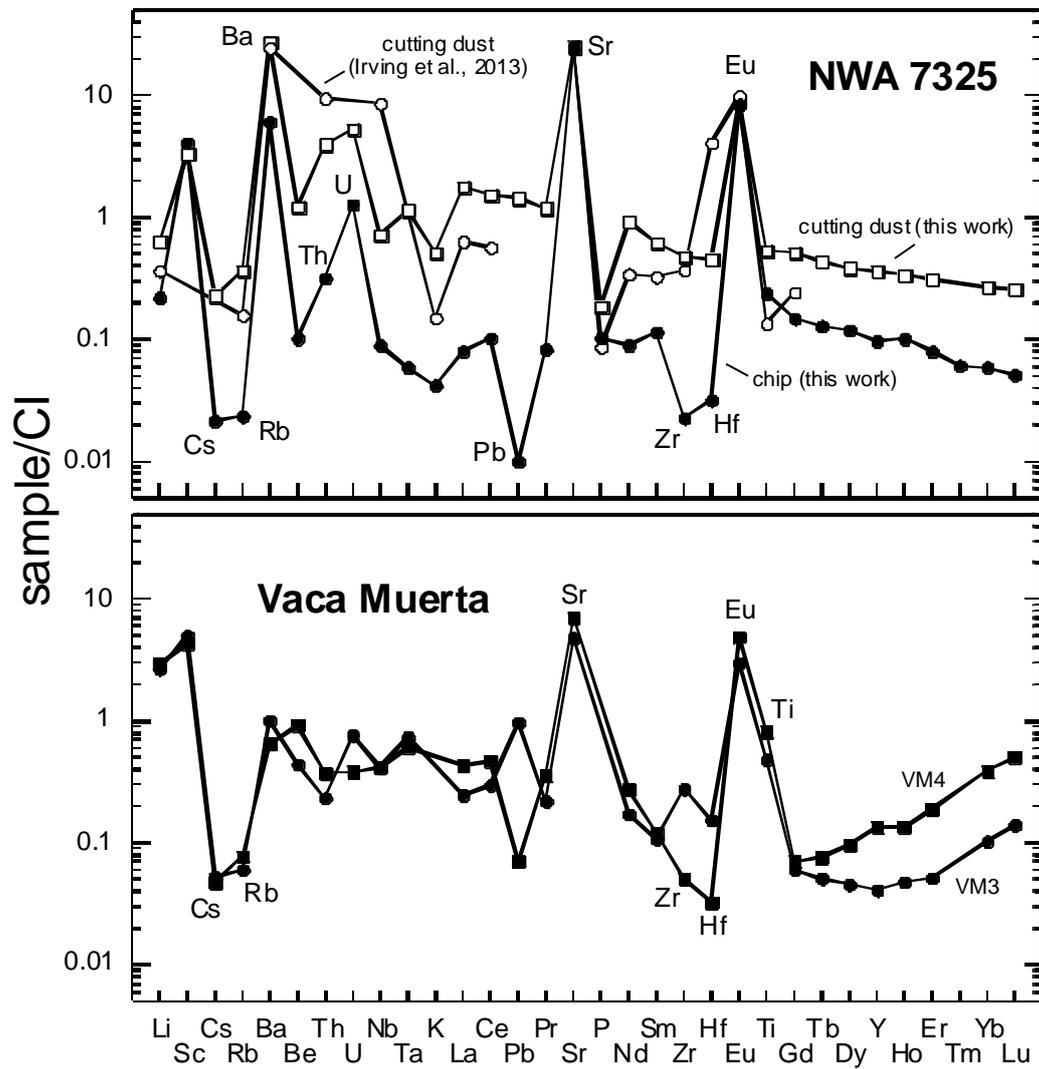
Figure 3. CI normalized multi-element patterns for NWA 7325 and two low-Ti gabbros from the Vaca
Muerta mesosiderite. The reference CI chondrite is from Barrat et al. (2012).

641

642

643

644
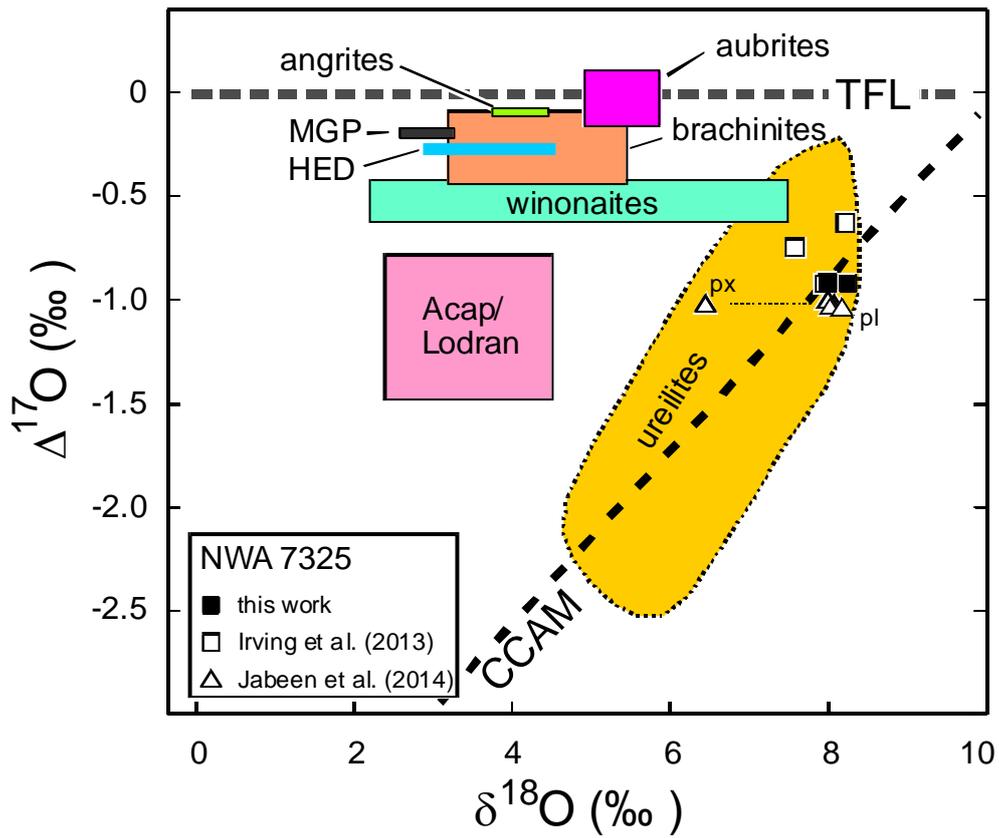
Figure 4. Oxygen isotope composition of NWA 7325 (Irving et al., 2013; Jabeen et al., 2014 and this work) compared with ureilites (Clayton and Mayeda, 1996) and other achondrites (Greenwood et al. 2012, 2014 and references therein). MGP, main-group pallasites; HEDs, howardites, eucrites, diogenites; TFL, terrestrial fractionation line; CCAM, the carbonaceous chondrite anhydrous mineral line (Clayton and Mayeda, 1999); Px, pyroxene; Pl, plagioclase.
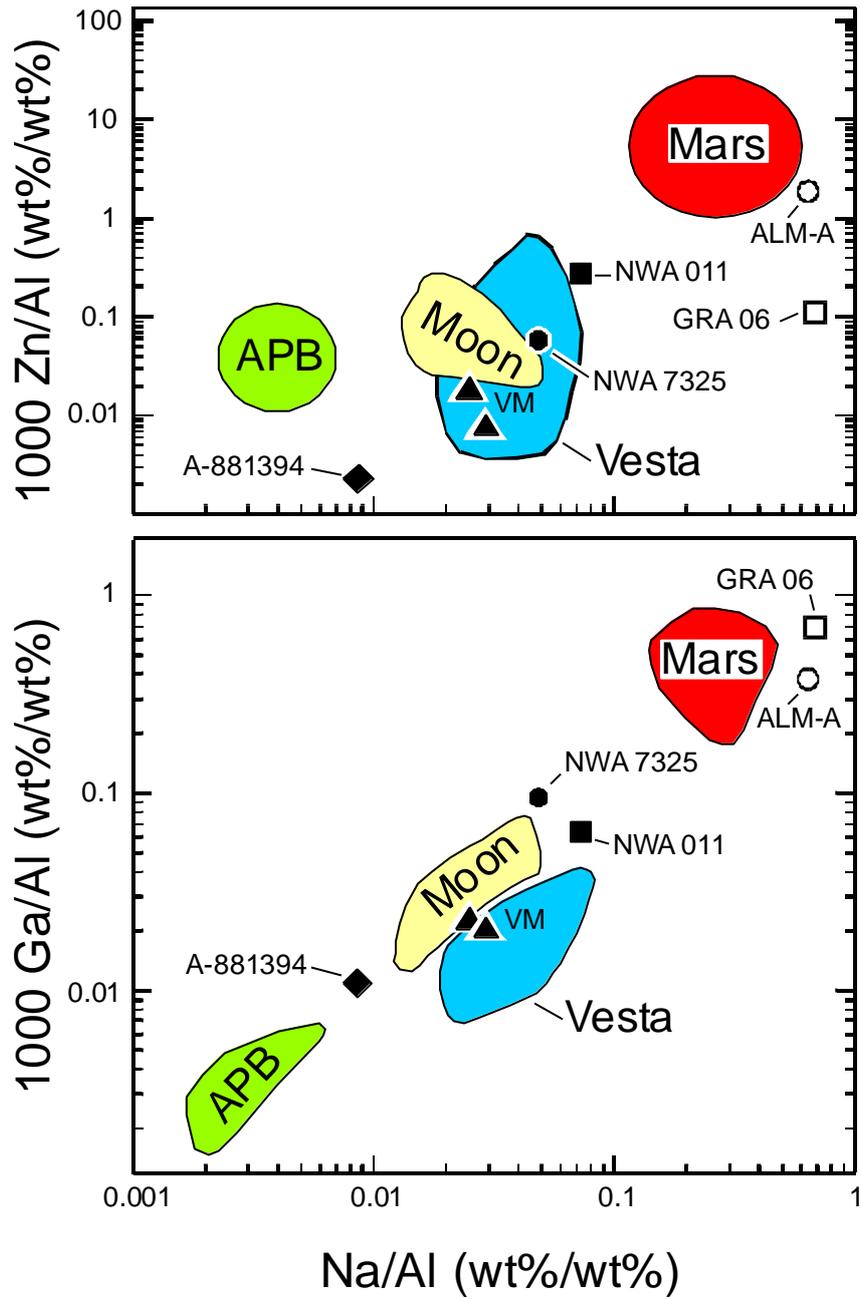
645
646
647
648
649
650
651
652
653
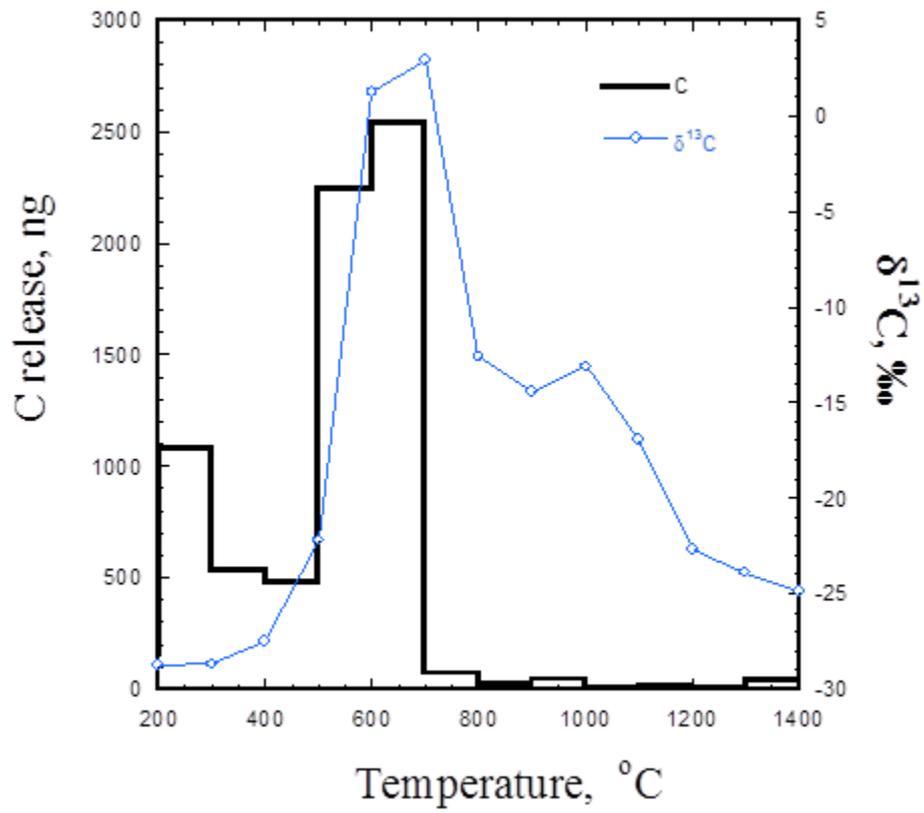
654
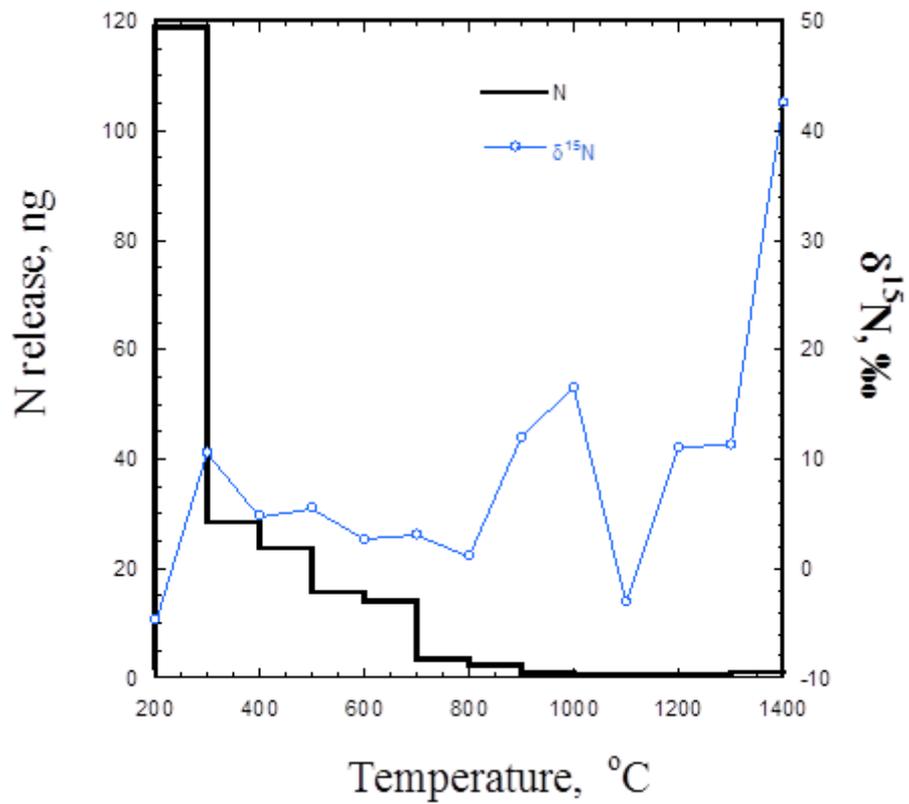
655

656   Figure 5. a: Carbon stepwise combustion results for NWA 7325; b: Nitrogen stepwise combustion results
657   for NWA 7325.
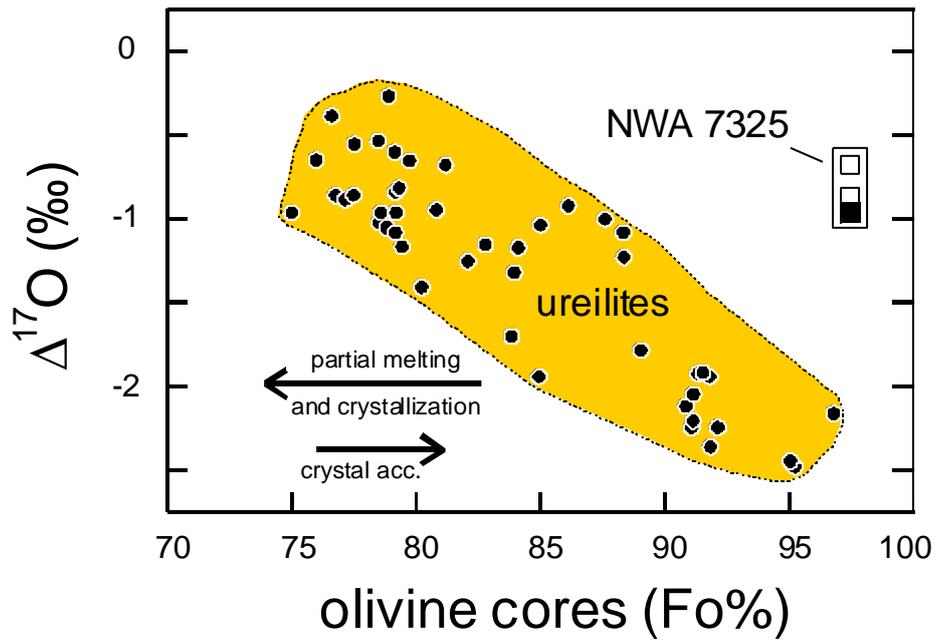
Figure 6. Plot of $\Delta^{17}O$ in the bulk rocks *vs.* olivine core compositions for ureilites (data from Clayton and Mayeda (1996), Downes et al. (2008), Singletary and Grove (2003), Goodrich et al. (2006, 2014) and references therein) and NWA 7425 (Irving et al., 2013 and this work, same symbols as Fig. 3).

Figure 7. Ga/Al, and Zn/Al vs. Na/Al plots comparing NWA 7325 (chip) and the two Vaca Muerta Pebbles (VM) with main types of achondrites (fields and data from Warren et al. (2013), Yamaguchi et al. (2002), Day et al. (2012) and Bischoff et al. (2014)). APB, angrite parent body.
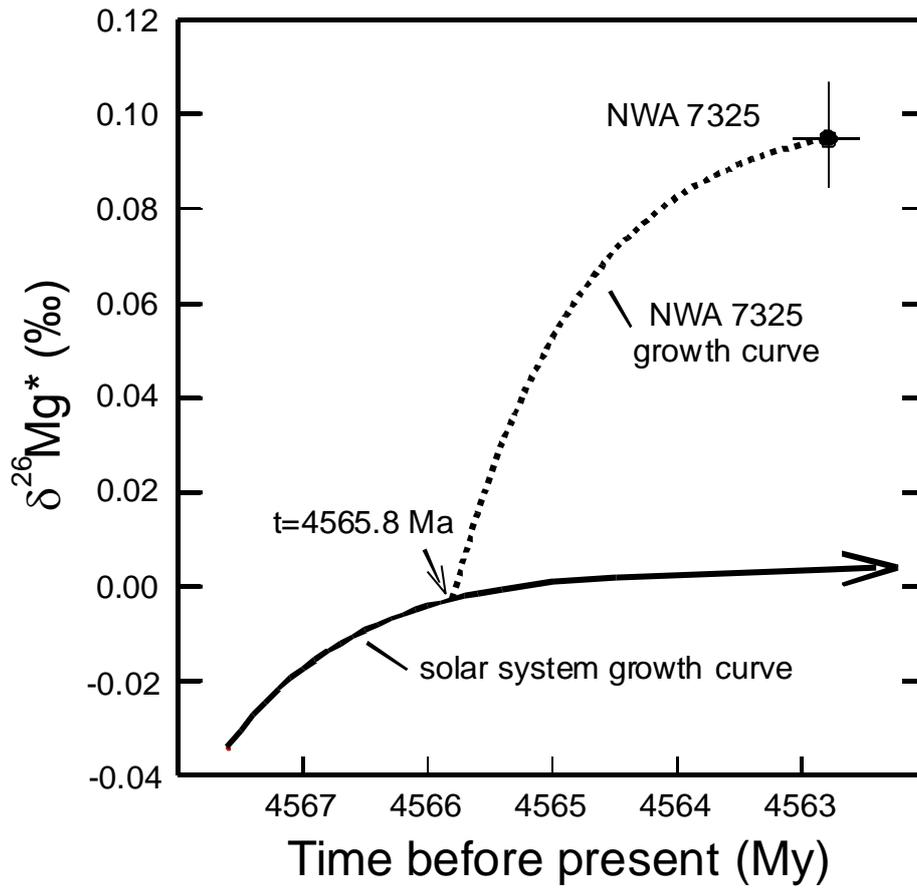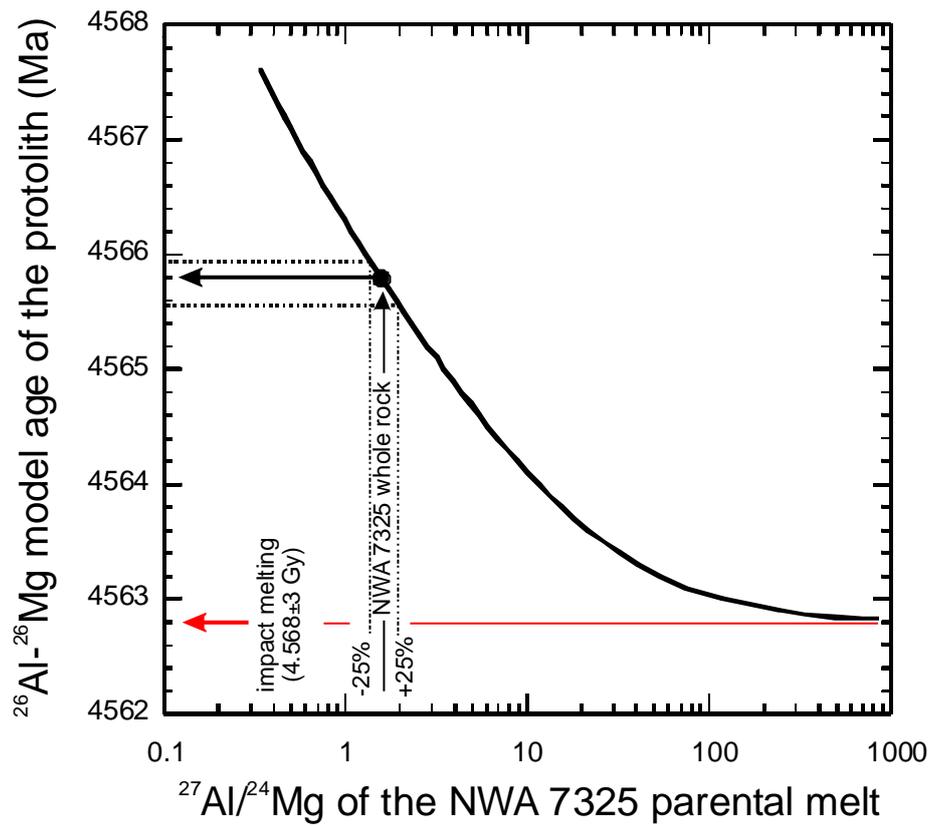
668

669 Figure 8. The Mg isotopic composition of NWA 7325 (Dunlap et al., 2014) compared to the
670 theoretical evolution of the Mg isotopic composition of the solar system (calculated for a chondritic
671 $^{27}Al/^{24}Mg$ ratio of 0.101, a $(^{26}Al/^{27}Al)_0$ of 5.23 x 10^{-5}, and a $\delta^{26}Mg*_0$ of -0.034 ‰ (Jacobsen et al.,
672 2008)).

673

674

675

676

677 Figure 9. Model age of the protolith of NWA 7325 vs. $^{27}Al/^{24}Mg$ of its parental melt. Assuming that
678 the parental melt and the whole rock have the same Al/Mg ratios ($^{27}Al/^{24}Mg= 1.56$), an intercept with
679 the solar system growth curve at about 4566 Ma is obtained.

680

681

682